JOURNAL OF QUATERNARY SCIENCE (2005) **20**(7–8) 821–838

Published online in Wiley InterScience (www.interscience.wiley.com). DOI: 10.1002/jqs.980

Equilibrium-line altitudes during the Last Glacial Maximum across the Brooks Range, Alaska

NICHOLAS L. BALASCIO,[1] DARRELL S. KAUFMAN[1]* and WILLIAM F. MANLEY[2]
[1] Northern Arizona University, Department of Geology, Flagstaff, AZ, USA
[2] University of Colorado, Institute of Arctic and Alpine Research, Boulder, CO, USA

Balascio, N. L., Kaufman, D. S. and Manley, W. F. 2005. Equilibrium-line altitudes during the Last Glacial Maximum across the Brooks Range, Alaska. *J. Quaternary Sci.*, **Vol. 20** pp. 821–838. ISSN 0267-8179.

Received 1 June 2005; Revised 18 September 2005; Accepted 21 September 2005

JQS Journal of Quaternary Science

ABSTRACT: Equilibrium-line altitudes (ELAs) were estimated for 383 reconstructed glaciers across the Brooks Range, northern Alaska, to investigate their regional pattern during the Last Glacial Maximum (LGM). Glacier outlines were delimited based on published field mapping and the original interpretations of aerial photographs. Glacier margins were digitised from 1:63 360-scale maps into a geographic information system (GIS) with a digital elevation model on a 60-m grid. ELAs were calculated for each reconstructed glacier using the accumulation area ratio method (AAR = 0.58). The analysis was restricted to relatively simple cirque and valley glaciers that deposited clearly identifiable LGM moraines, and that did not merge with the complex transection glacier ice that filled most troughs of the range. The glaciers used in this analysis had areas ranging from 0.14 to 120 km^2. Their ELAs rose from 470 m a.s.l. in the western Brooks Range to 1860 m a.s.l. in the east, over a distance of 1000 km. The ELAs were fitted with a third-order polynomial trend surface to model their distribution across the range, and to investigate the source of local-scale variations. The trend surface lowers toward the west and south, similar to previously derived trends based on glaciation thresholds. In addition, ELAs in the northeastern part of the range lower northward toward the Beaufort Sea, which has not been reported as strongly in other studies. Modern glacier ELAs also lower toward the southwest. The depression of LGM ELAs from modern glacier ELAs is greatest in the central Brooks Range (a maximum of 700 m), and decreases to the east (200 m). The regional pattern of LGM ELAs points to the primary source of moisture from the North Pacific, as it is today. The unexpected trend of LGM ELAs in the northeast part of the range is supported by recent field mapping, where anomalous ice distribution and ELAs reflect complicated LGM climate patterns and possibly late Quaternary tectonism. Copyright © 2005 John Wiley & Sons, Ltd.

KEYWORDS: equilibrium-line altitude; Brooks Range; Last Glacial Maximum; Alaska.

Introduction

The equilibrium-line altitude (ELA) of mid- and high-latitude alpine glaciers is controlled mainly by summer temperatures and winter precipitation. Reconstructing the ELA of palaeoglaciers on the basis of geomorphic evidence provides a quantitative means of interpreting past climate during former intervals of presumed steady-state conditions. The regional trend of reconstructed ELAs can be examined to infer past atmospheric circulation and temperature patterns, because the ELA gradient lowers toward accumulation-season moisture or cold ablation-season temperatures. Differences between the ELAs of extant glaciers and those reconstructed from Pleistocene moraines reflect differences between present and full-glacial atmospheric conditions. The geometry of the ELA trend surface can itself be used to investigate the controls on ELAs. Although summer temperature and winter precipitation are most important, factors such as aspect, slope, shading, size, shape, and local geography of a glacier may cause an ELA to be above or below the regional trend. Relationships between the magnitude of the deviation of glaciers from the regional trend and the physiographic characteristics of glaciers can be used to identify the factors that lead to local-scale perturbation of the ELA surface.

This study provides a detailed analysis of ELAs across the Brooks Range of northern Alaska. We focus on the maximum position of valley and cirque glaciers during the local Last Glacial Maximum (LGM), for which the morainal evidence is most clear for delimiting past glacier extent. A total of 383 reconstructed glaciers were digitised and analysed in two geographic information systems (GIS) to estimate their former ELAs. A trend surface was fitted to these data to model their spatial variation across the Brooks Range and to interpret the regional controls on ELAs in northern Alaska during the LGM. This record of ELAs for the Brooks Range refines the earlier work of

* Correspondence to: Darrell S. Kaufman, Department of Geology, Northern Arizona University, Flagstaff, AZ 86011, USA. E-mail: darrell.kaufman@nau.edu

Porter *et al.* (1983), whose analysis of glaciation thresholds provided a general illustration of climate patterns across northern Alaska during the LGM.

Setting

Except for the Cordilleran Ice Sheet in the south, Alaska during the LGM was largely unglaciated due to its isolation from major sources of moisture (Hamilton, 1994; Kaufman and Manley, 2004). Sea-ice cover reduced the moisture available from the north and west, and the exposure of the Bering/Chukchi Platform increased the continentality across central Alaska. Glaciation during the LGM in most of Alaska was therefore restricted to alpine areas. Ice was more extensive during the early part of the late Pleistocene when sea level was higher and global ice volume relatively low (e.g. Kaufman *et al.*, 2001).

The Brooks Range is ca. 1000 km long extending from west to east across northern Alaska. The range is highest in the east reaching over ca. 2700 m a.s.l. in elevation (Fig. 1). The north–south width of the range varies from ca. 180 to 200 km, with a total area of about 190 000 km^2. The western Brooks Range, ca. 90 km inland of the Chukchi Sea, consists of the De Long and Baird Mountains, while the central and eastern parts of the range form a single chain of mountains that trends west–east in the central Brooks Range and trends northeast toward the Beaufort Sea in the eastern Brooks Range.

The broad expanse and topographic diversity of the Brooks Range gives rise to a variety of climatic regimes. Because only a few weather stations are scattered around northern Alaska, descriptions of the climate of the Brooks Range are mainly characterised by regional summaries (Fahl, 1975; Péwé, 1975; Daly *et al.*, 1994; Mock *et al.*, 1998), and short-term climate investigations (Haugen, 1979; Wendler *et al.*, 1974, 1975). In the eastern and central parts of the range, the dominant temperature and precipitation gradients are from north to south (Manley and Daley, 2005). South of the divide, the climate is continental, with large temperature extremes, mean annual air temperatures (MAT) from −4 to −8 °C, and discontinuous permafrost. North of the divide, the climate is arctic, with MAT from −8 to −12 °C, and continuous permafrost (Péwé, 1975). Temperatures decrease north of the range toward the Beaufort and Chukchi Seas (Haugen, 1979; Daly *et al.*, 1994). The western Brooks Range is more maritime, with temperatures from −7 to −9 °C. Mean annual precipitation generally decreases to the north and east across the range, from ca. 30 cm in the west to ca. 15 cm in the northeast, although gauges on McCall Glacier in the northeast (Wendler *et al.*, 1974, 1975) recorded mean annual precipitation of ca. 50 cm, between 1969 and 1972, much higher than in other parts of the range.

Modern glaciers are most numerous in the central Brooks Range, where they occupy the highest north-facing cirques. The eastern Brooks Range has the largest glaciers, which are up to 10 km in length around Mount Chamberlin and Mount Michelson (Fig. 1), where the range reaches its peak elevations. The elevation of modern glaciation thresholds increases from 1700 m a.s.l. in the west to 2300 m a.s.l. in the east, but decreases to 2000 m a.s.l. in the northeast (Porter *et al.*, 1983). The trend of modern glacier thresholds is similar to the trend of precipitation, which indicates that presently, moisture availability strongly influences the distribution of glaciers across the Brooks Range.

Pleistocene glaciers covered most of the central and eastern Brooks Range, and parts of the De Long and Baird Mountains in the west (Fig. 1). Glaciers formed at lower elevations in the western Brooks Range, and large transection glaciers (interconnected systems of large, low-lying valley glaciers with poorly defined ice divides) occupied most of the major river valleys in the central and eastern Brooks Range. Late Wisconsin glaciation thresholds in the western Brooks Range decreased in elevation toward the southwest to 900 m a.s.l., and rose to

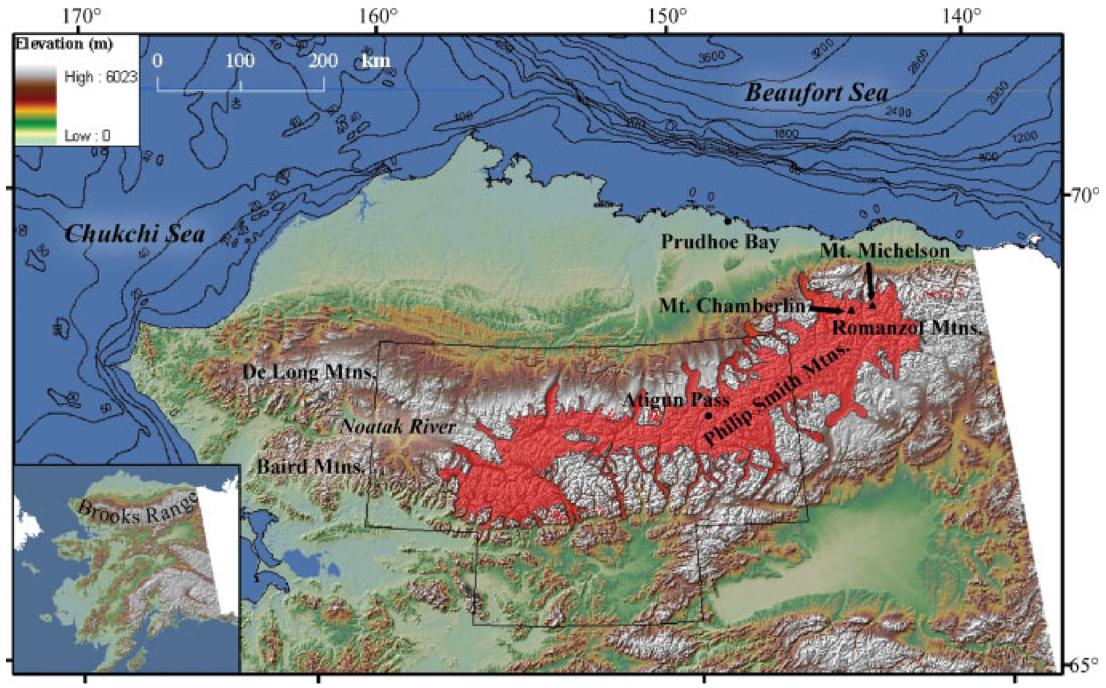

Figure 1 Shaded relief map of northern Alaska showing the extent of glacier ice (in red) during the Last Glacial Maximum across the Brooks Range (Kaufman and Manley, 2004) and the bathymetry (m) of the continental shelves of the Chukchi and Beaufort Seas. Black solid line indicates the extent of surficial geologic mapping by Hamilton (1978a, 1978b, 1979a, 1979b, 1980, 1981, 1984a, 1984b, 2002a, 2002b, 2003)

2100 m a.s.l. in the eastern Brooks Range, where the gradient of the trend shifted to a more southerly orientation (Porter *et al.*, 1983).

The Pleistocene glacial geology of the Brooks Range is reviewed by Hamilton (1986, 1994). We rely on his subdivision of glaciations and age control in this study. In the Brooks Range, Late Pleistocene glacier advances are nominally assigned to the Itkillik glaciation, and are divided into the Itkillik I glaciation (early Wisconsin *sensu lato*), and the Itkillik II glaciation, which constitutes the local LGM and is coeval with the late Wisconsin. During the Itkillik II glaciation, glaciers were less extensive than during the Itkillik I glaciation. Itkillik II ice reached only 25 km north of the Brooks Range, compared to Itkillik I ice that extended 40 km north of the range. The age of the Itkillik II glaciation is bracketed between 24 and 15 ka. Itkillik II drift is characterised by topographically irregular deposits that are steeper, more bouldery, and less vegetated than drift of Itkillik I age. Moraines have multiple crests and other primary constructional features and greater relief than moraines of Itkillik I age. A readvance of Itkillik II ice occurred between 13 and 11.5 ka (Hamilton, 2003). This advance left distinctive moraines that are morphologically similar to deposits of the Itkillik II glacial maximum. Glaciers extended up to 15–20 km north of the range front in some valleys and less extensive moraines in other valleys.

Methods

Our investigation of ELAs proceeded in four steps. (1) The extent of Itkillik II glaciers were reconstructed on the basis of glacial geomorphic evidence interpreted from aerial photographs and observed in the field. (2) Palaeoglacier outlines were digitised into a GIS to calculate and display spatial variations of glacier physical attributes. (3) A three-dimensional trend surface was created to express the variability of ELAs across the Brooks Range. And (4) the residual values (the deviation of palaeoglacier ELAs from the trend surface) were compared with glacier attributes to infer local factors influencing ELAs.

Identifying and reconstructing LGM glaciers

Ninety per cent of the 383 palaeoglaciers were reconstructed by interpretation of aerial photographs, and about 10% were checked by field observations. All were cirque and valley glaciers situated above or beyond, but not confluent with, the larger transection ice that filled the valleys within most of the Brooks Range. These smaller palaeoglaciers provide simpler systems for which the division between the accumulation and ablation area is more easily defined, therefore allowing the ELA to be derived more confidently. The 383 palaeoglaciers include nearly all of the LGM valley and cirque glaciers that could be located. Gaps in the spatial distribution of the glaciers across the range reflect the absence of cirque and valley glaciers during the LGM.

The accuracy of the ELA analysis depends on the ability to identify confidently LGM glacial landforms, and on the consistency of techniques used to map palaeoglacier outlines. The location of LGM moraines used to reconstruct the former glaciers began with Hamilton's 1:250 000-scale surficial-geologic maps, which cover most of the central Brooks Range (Fig. 1) (Hamilton, 1978a, 1978b, 1979a, 1979b, 1980, 1981, 1984a, 1984b, 2002a, 2002b, 2003). LGM glaciers in the western and eastern Brooks Range, not covered by Hamilton's mapping, were mapped for this study from aerial photographs and field observations (Balascio, 2003; Balascio *et al.*, in press). All reconstructed palaeoglacier outlines were then plotted onto 1:63 360-scale topographic maps.

Glacial erosional and depositional features ascribed to the Itkillik II glaciation are typically well expressed in aerial photographs. Cirques last occupied by Itkillik II glaciers are backed by fresh, steep headwalls, and relatively level cirque floors, and moraines exhibit sharp crests and hummocks. The outlines of palaeoglaciers were reconstructed using these cirque and moraine morphologies as well as trimlines, when visible, to infer ice thickness. Consistency among palaeoglacier reconstructions was maintained by assuming uniform up-glacier ice thickness, and that cirques were completely filled with ice by drawing the upper limit generally following the highest most continuous contour of the cirque headwall. Although some subjectivity is involved from cirque-to-cirque, the accuracy of this measurement has little effect on the area of the glacier because of the steepness of cirque headwalls. Because moraines of late Itkillik II and maximum Itkillik II are morphologically similar, the two might have been confused in some valleys, which would result in erroneously high ELAs. However, Hamilton distinguishes between late Itkillik II and LGM moraines in most areas, and our interpretations generally follow his extensive field-based work.

The spatial density of the 383 palaeoglaciers used in this study is somewhat less than has been used in previous studies. For the Brooks Range, the density is approximately two palaeoglaciers per 1000 km^2 in an area of ca. 190 000 km^2, with 47 palaeoglaciers in the eastern, 228 paleoglaciers in the central, and 108 palaeoglaciers in the western Brooks Range. Similar studies in other mountain ranges were based on slightly higher concentrations of data points (glacier ELAs or glaciation threshold elevations). For example, Hawkins' (1985) study of the Merchants Bay area, Baffin Island, was based on 14 points per 1000 km^2 in an area of 2500 km^2, Leonard's (1984) study of the San Juan Mountains, Colorado, was based on four points per 1000 km^2 in an area of 22 500 km^2 area, and Locke's (1990) study of western Montana was based on three points per 1000 km^2 in an area of 176 000 km^2.

GIS analysis

The GIS made it possible to easily calculate a variety of physical characteristics for many glaciers and provided a means of clearly illustrating spatial data across a broad area. Two software packages were used: ArcGIS and MFWorks. GIS procedures were developed to calculate former ELAs and glacier attributes from mapped glacier outlines using 60-m grid digital elevation models (DEMs), ArcGIS commands, and the MFWorks scripting language. The surfaces of the former glaciers were interpolated from the digitised glacier outlines and used to calculate the ELA, area, slope, aspect, perimeter, and volume for each palaeoglacier. Compactness was also calculated ($4\pi A/P^2$, where A = area and P = perimeter), and is a non-dimensional measure of circularity ranging from 0.0 for a straight line to 1.0 for a circle (Allen, 1998). Similar geospatial analyses of glaciers are presented in Manley (in press).

Errors are associated with the transfer of palaeoglacier outlines to digital format and the interpolation of palaeoglacier surface elevations used to derive the ELA. Errors with the use of GIS stem from the DEMs, which are the basis for calculating the physical characteristics of glaciers. The United States

Geological Survey standards for the DEMs used in this study have root-mean-squared (RMS) errors of less than one-half of the contour interval (RMS ca. 10–15 m). Greater uncertainty is probably associated with the subjectivity of reconstructing glacier outlines, which was minimised by applying consistent techniques to outlining former glaciers.

The variety of methods used to reconstruct former ELAs was recently summarised by Benn *et al.* (2005). In this study, palaeo-ELAs were estimated on the basis of the accumulation area ratio method (AAR), which has been shown to produce consistent results (Porter, 2001). This method assumes a fixed ratio between the accumulation and ablation areas of a glacier. Different ratios have been applied, ranging from 0.5 to 0.8, although most use 0.60–0.65. We used a recently derived ratio of 0.58, which is based on a global analysis of average AARs for steady-state mass balance of modern glaciers (Dyurgerov, pers. comm.; see Dyurgerov, 2002). To determine how much the choice of an AAR affects the estimated ELA, we applied a range of AAR values in a sensitivity analysis. The results from the Brooks Range glaciers analysed in this study show that, by changing the inferred AAR by $\pm$ 0.1, the average ELA changes by only $\pm$ 35 m (Balascio, 2003), which is small compared to the overall ELA gradient, and the LGM ELA depression. Similarly, if the inferred AAR varied with climate across the region, we argue that the influence would be secondary to the overall trend of ELAs, and to more important local factors involving debris cover and topographic shielding. Regardless of the accuracy of the ELA value, the choice of an AAR does not impact the first-order spatial trends that are the focus of this study.

The map of ELAs was then used to create three-dimensional surfaces to represent the ELA distribution across the Brooks Range. In the GIS, each glacier was represented by its ELA at a single point. These single points, or 'centroids', were located by GIS scripting at the approximate midpoint of the glacier's long and short axes. ELAs were then contoured and fit with first through fourth order polynomials to examine the goodness-of-fit of progressively higher-order polynomials. Residual values were calculated for each glacier to statistically compare the trend surfaces. The residual values were regressed against each glacier characteristic to identify significant relationships.

Results and discussion

Palaeo-ELAs

The distribution of the 383 reconstructed glaciers is not uniform across the range (Fig. 2). LGM cirque and valley glaciers in the Brooks Range were clustered on the edge of the range, especially in the south where snowline intersected the landscape, but where ice did not smother the mountains as it did near the crest of the range. In addition, there is a gap in former cirque and valley glaciers between the central and northeastern Brooks Range in the Philip Smith Mountains. The north-to-south distribution of data points is also limited in the east, where the mountains held extensive transection glaciers.

Reconstructed LGM cirque and valley glaciers vary in size, shape, and elevation (Table 1), with areas ranging from 0.14 to 120 km^2, compactness from 0.03 to 0.71, slope from 4° to 30°, and volume from 0.002 to 17 km^3. Glacier aspects range in all directions, although 93% are north-facing between 280° and 80°, with only 26 glaciers facing more southerly. The locations and physical characteristics of all of the glaciers reconstructed in this study are listed in the Appendix.

Palaeo-ELAs rise from west to east across the Brooks Range (Fig. 2). The rise appears to occur in two major steps, one with a slope of 3.8 m km^{-1} at ca. 155° W longitude, and the other with a slope of 3.3 m km^{-1} at 144° W. Alternatively, the lack of ELA change in the area separating these steps might result from the sparse data coverage in this zone. LGM ELAs increase from 470 m a.s.l. in the De Long Mountains to 1860 m a.s.l. in the Romanzof Mountains. Generally, ELAs tend to be higher over the highest massifs and lower over the Noatak Basin and along the southern range front. The palaeo-ELAs decrease in

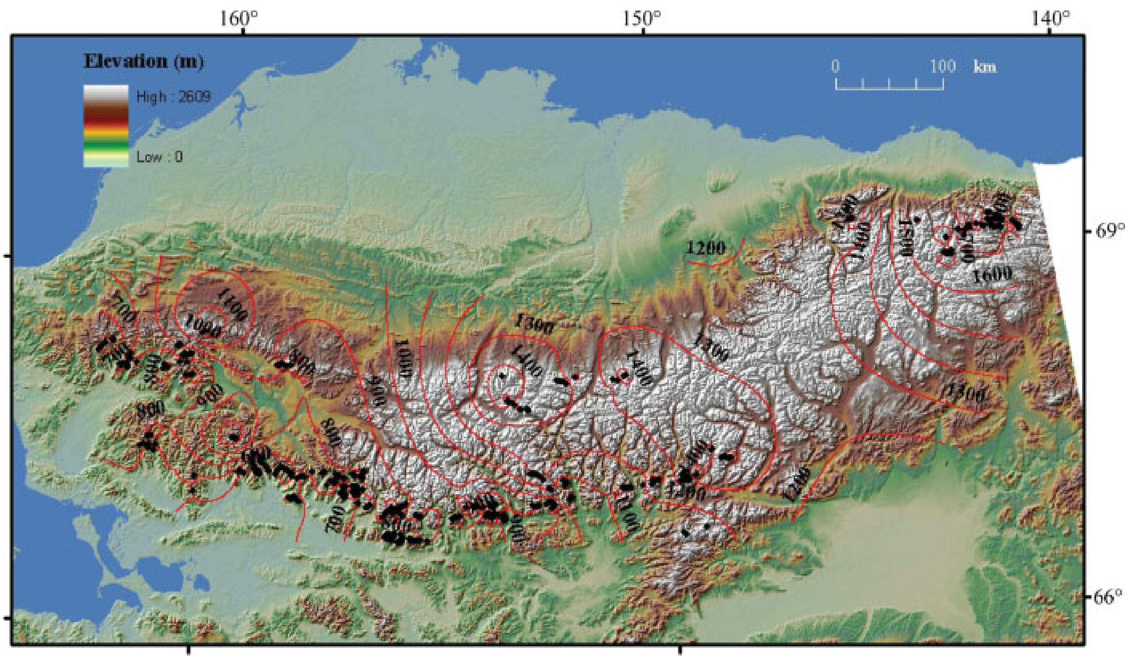

Figure 2 Contoured equilibrium-line altitudes for 383 Last Glacial Maximum valley glaciers across the Brooks Range. Black dots show the location of reconstructed glaciers. Contours were generated using a geographic information system interpolation method (Balascio, 2003). Contour interval is 100 m

Table 1 Summary of physical characteristics of reconstructed Last Glacial Maximum valley glacier ($n = 383$)

	Minimum	Maximum	Median	Average $\pm$ 1 σ
Slope (°)	4	30	11	12 ± 4.4
Area (km^2)	0.14	120	0.84	2.3 ± 6.9
Volume (km^3)	0.002	17	0.05	0.19 ± 0.89
Compactness[a]	0.03	0.71	0.43	0.41 ± 0.14
Length (km)	0.40	12.7	1.4	1.9 ± 1.5
ELA (m)	468	1859	854	963 ± 325

[a]Measure of circularity ($4\pi A/P^2$, where A = area and P = perimeter).

the northeasternmost part of the range, from 1600 to 1700 m a.s.l. over the Mount Michelson and Mount Chamberlin areas, to 1500 m a.s.l. in the eastern Romanzof Mountains. Locally anomalous palaeo-ELAs result in isolated high contours, especially in the western Brooks Range, whereas analogous areas of isolated low contours are not seen.

Trend surfaces

Statistically fit trend surfaces were calculated for palaeo-ELAs across the Brooks Range to find the surface that best represents the regional variability of ELAs. Regional-scale changes refer to trends on the order of hundreds of kilometres that reflect the broad pattern of climate that controls ELAs, as opposed to local-scale changes that reflect topographic, or geographic effects at scales of tens of kilometres. Four trend surfaces were calculated (Balascio, 2003). A first-order fit created a planar surface that slopes to the southwest (230°) from 1700 to 600 m a.s.l., at 1.1 m km^{-1}. The second-order polynomial created a surface that ranges in elevation from 500 to 1800 m a.s.l., with a broad ridge dividing the southwestern dip of the palaeo-ELA surface in the central and western Brooks Range from the northwestern dip of the palaeo-ELA surface in the eastern Brooks Range. The surface slopes gently (ca. 1.3 m km^{-1}) along the north flank of the western and central Brooks Range and steeper (ca. 2.6–4.0 m km^{-1}) along the southern flank of the range. The trend surface maintains a southwestern dip from west to east along the southern flank of the range. In the northeastern Brooks Range the surface slopes uniformly at ca. 3.3 m km^{-1}. The third-order polynomial (Fig. 3) exhibits a sharper ridge that more closely follows the crest of the range. Along the southern flank of the range, this surface forms a trough extending from west to east, more closely following the actual palaeo-ELA values. ELA gradients range from ca. 1.4 to 13 m km^{-1}, with the steepest portion of the surface dipping north in the northeastern Brooks Range. In the western Brooks Range the surface faces southward, similar to the second-order fit, but exhibits a progression to a southern dip eastward across the range. In the northwest corner of the range, the surface dips north, but this trend is supported by few data points. A fourth-order surface was created and infers even greater changes between palaeo-ELAs of closely spaced glaciers, with slopes ranging up to 13.5 m km^{-1}.

The contoured palaeo-ELA data together with goodness-of-fit statistics were used to determine which modelled surface best represents the regional variability of ELAs across the Brooks Range. Visual comparison of the contoured palaeoELA data shows that the third-order trend surface best coincides with the major (100-km-scale) trends in the ELAs across the Brooks Range. RMS and chi-squared statistics show that increasing polynomial orders yields diminishing benefits (Table 2). At orders higher than third order, differences in RMS and chi-squared values between the surfaces are minor. We therefore elect to represent the regional palaeo-ELA across the Brooks Range using a third-order trend surface.

The contoured trend surface of the LGM ELAs is broadly similar to Porter *et al.*'s (1983; their Fig. 4–4) contoured LGM glaciation threshold altitudes for the Brooks Range. As expected, the ELAs (600–1800 m a.s.l.) are systematically lower than glacial thresholds (900–2100 m a.s.l.), because glaciation thresholds are commonly 100–200 m above ELAs (Meierding, 1982). Both the glaciation threshold and the ELA surfaces decrease toward the southwest in the western part of the range. In the central Brooks Range, glaciation thresholds dip toward the south whereas the ELA trend surface maintains a southwestern dip across the range. In the northeastern Brooks Range, ELAs decline toward the north and slightly to the east, a trend that is incongruent with the rest of the range and that is not exhibited as strongly from glaciation threshold interpretations. Porter *et al.* (1983) show a slight lowering to the north, indicated by their single-dashed contour just west of Mount Chamberlin.

The palaeo-ELAs in the northeastern Brooks Range are supported by detailed, on-the-ground, glacial-geologic field mapping (Balascio, 2003; Balascio *et al.*, in press). They are unexpected because ELAs typically rise in the lee side of a mountain range in response to precipitation shadows. The lower ELAs reconstructed for the northeasternmost glaciers probably reflects their proximity to the Beaufort Sea, where summer temperatures are lower in response to a shorter duration of seasonally open water.

Residual values

Residual values were used to explore relationships between the physical characteristics of the palaeoglaciers and their deviation from the trend surface. Residuals were calculated as the difference between the palaeo-ELA derived from the AARs and the modelled value derived using the coordinates for each glacier centroid and the third-order polynomial. The spatial and frequency distributions were studied to identify the factors that may influence the residual values. The frequency of residual values is evenly distributed above and below the trend surface (Fig. 4). Furthermore, there are no systematic regional trends in residual values, indicating that either our choice of a single AAR value across the range was appropriate or, if not, then at least the residual values are not biased by the assumption of a uniform AAR. The average of the absolute value of the residuals is 91 ± 77 m, similar to the RMS. Spatially, the highest residuals coincide with the highest massifs (Balascio, 2003). This relation is also expressed by the tendency ($p < 0.01$; Table 3) for residual values to be higher for glaciers at higher elevations. High ELAs in the tallest massifs of a range have also been found by others (Leonard, 1984; Locke, 1990), and interpreted to represent moisture diversion around the highest parts of the ranges.

Palaeoglacier ELAs also deviate from the regional trend as a function of glacier size, perhaps for the same reason. Although most mapped glaciers were small (ca. 60% with areas less than 1 km^2; ca. 70% with volumes less than 0.1 km^3; ca. 65% with lengths less than 2 km), the inverse relations of area and volume to residual value, and the positive relations of slope and compactness to residual value demonstrate a significant ($p < 0.01$) relationship between glacier size and residual value (Table 3). These four characteristics all relate to the size of a glacier and covary (e.g. area and volume). In most cases, the slope of a

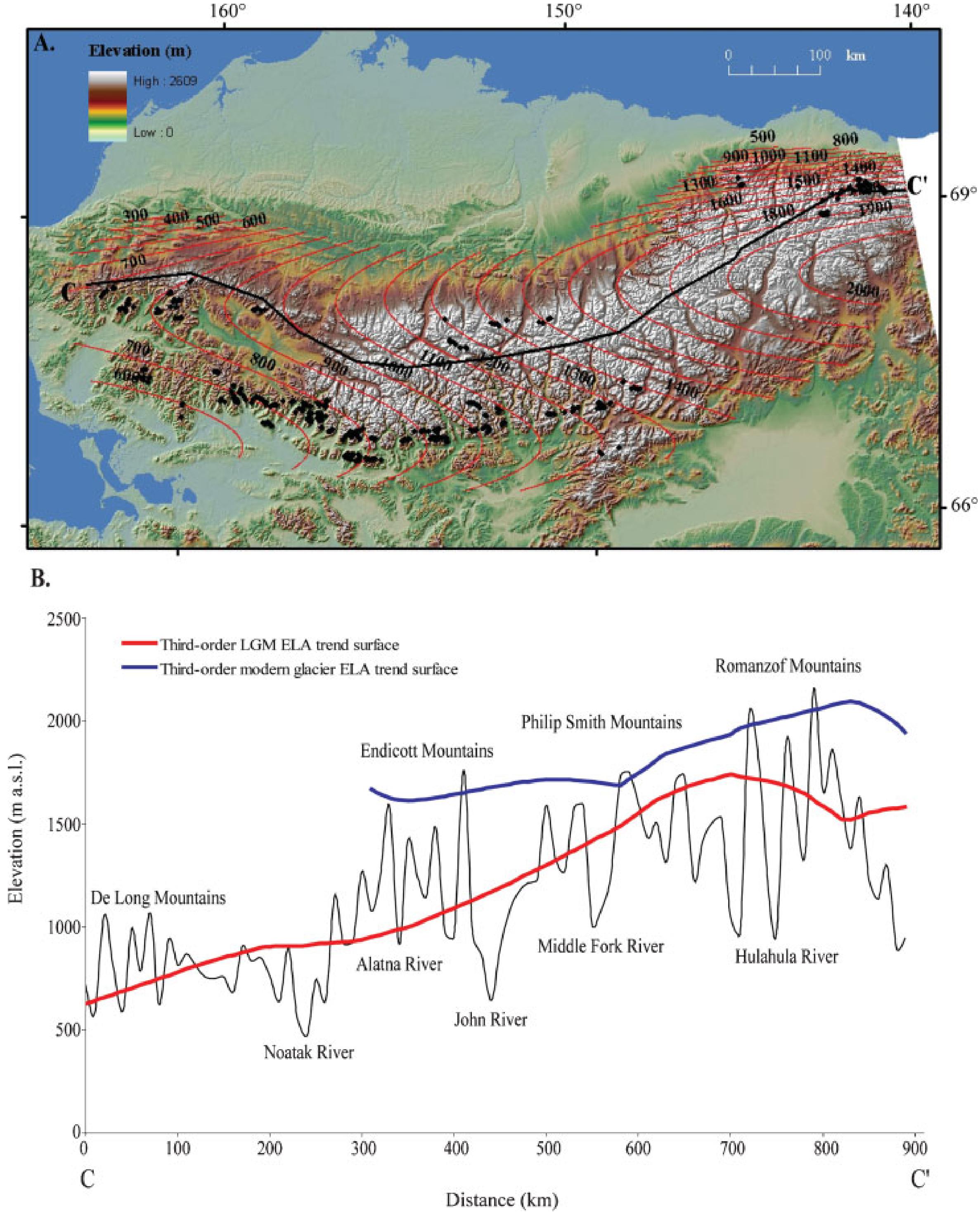

Figure 3 Reconstructed equilibrium-line altitude (ELA) surface for the Last Glacial Maximum across the Brooks Range. (A) Relief map of the Brooks Range showing contours of the third-order trend surface and the location of glaciers used to create the surface (black dots). (B) Topographic profile from C to C′ across the crest of the Brooks Range showing the ELA surface in relation to local relief and the modern glacier ELA third-order trend surface

glacier is related to the size of a glacier because smaller glaciers (less than ca. 2 km^2) occupy the heads of valleys within the steep peaks of mountains. Larger glaciers extend farther down-valley and flow onto and erode troughs with lower slopes. Compactness is a measure of a glacier's circularity, and clearly distinguishes between long, linear valley glaciers and more rounded cirque glaciers. Regressions of these characteristics show that smaller LGM glaciers tend to lie above the regional ELA trend surface. This is somewhat unexpected because previous work has shown that small glaciers sheltered in deeply eroded cirques, shaded by steep headwalls typically persist at lower altitudes than their larger neighbours (Clark *et al.*, 1994). Similarly, the ELA would have been lower for debris-covered glaciers, which might have been more prevalent at higher elevations. The tendency for small glaciers to lie above the ELA trend surface may reflect the drying of air masses at higher elevation. The effect of orographic uplift of air on limiting glacier size may be stronger than the beneficial shading effects of deep cirques. Although this trend may represent a local-scale climate effect, the relation between residual value and glacier size is not strong, as indicated by the low R^2 values.

Table 2 Summary statistics for equilibrium-line altitude trend-surface fits of four different polynomial orders

Order[a]	RMS[b] (m)	χ^2
1st	157	9.39E + 06
2nd	133	6.75E + 06
3rd	119	5.41E + 06
4th	115	5.03E + 06

[a] $y = b + x_1 + x_2 = T_1$
$y = T_1 + x_1^2 + x_1x_2 + x_2^2 = T_2$
$y = T_2 + x_1^3 + x_1^2x_2 + x_1x_2^2 + x_2^3 = T_3$
$y = T_3 + x_1^4 + x_1^3x_2 + x_1^2x_2^2 + x_1x_2^3 + x_2^4 = T_4$
[b] RMS = root mean squared.

Aspect also covaries with residual value, although only weakly (Table 3). The relationship between glacier aspect and deviation from the regional ELA trend is expected because glaciers that face toward the north are more shaded from solar radiation than those facing south, and tend to have lower ELAs. Generally, the south-facing glaciers have ELAs that are above the regional trend rather than below it, although there are a few north-facing glaciers with high residual values and a few south-facing glaciers with low residual values.

Implications for LGM atmospheric circulation across Alaska

The ELAs of modern glaciers in the Brooks Range were examined to compare with the trends from the palaeoglaciers. Modern ELAs were determined using similar methods to those used to estimate LGM ELAs. Modern glacier ELAs were estimated using an AAR of 0.58 applied to 940 glacier outlines taken from USGS 1:63 360-scale topographic maps and with USGS DEMs derived from the same maps. The modern glacier ELA data were also fit with a third-order polynomial trend surface to represent their regional variation.

The southwest-sloping regional palaeo-ELA trend is similar to the overall trend of the modern glacier ELAs across the Brooks Range (Fig. 3). The similarity indicates that, like today, LGM mountain glaciers in the Brooks Range were strongly influenced by moisture availability, which was supplied dominantly from the southwest. A southwest moisture source is also manifested by modern glacier ELAs that rise on the lee side of the central Brooks Range. In detail, the trend surface of modern glacier ELAs is lowest, and relatively horizontal at ca. 1600 m a.s.l. in the central Brooks Range. Modern ELAs rise to 2100 m a.s.l. as summit elevations increase in the eastern Brooks Range.

The difference between modern and LGM ELAs (= ΔELA) was larger in the central Brooks Range (a maximum of ca. 700 m) than in the eastern Brooks Range (ca. 200 m) where glacier elevations are higher (Fig. 3). This minor depression in the eastern Brooks Range may indicate the influence of postglacial tectonic uplift that elevated moraines locally (Porter *et al.*, 1983). The rapidity of uplift would have been remarkable, however, and without significant geomorphic evidence of postglacial tectonic activity. The tendency toward lower ΔELA values with increasing glacier elevation has been documented elsewhere (e.g. Mark *et al.*, 2005), and has been attributed to the influence of basin morphometry on the response of glaciers to climatic change. Alternatively, the eastward decrease in ΔELA might indicate increased Holocene sea-surface temperatures and reduced sea ice that allow moisture from the Beaufort Sea to nourish glaciers inland and to lower modern glacier ELAs (Balascio *et al.*, in press).

The magnitude of LGM ELA lowering in the Brooks Range is similar to other parts of Alaska where values are typically ca. 300–600 m (Hamilton and Porter, 1975; Kaufman and Hopkins, 1986; Mann and Peteet, 1994; Stillwell and Kaufman, 1996; Manley *et al.*, 1997; Briner and Kaufman, 2000).

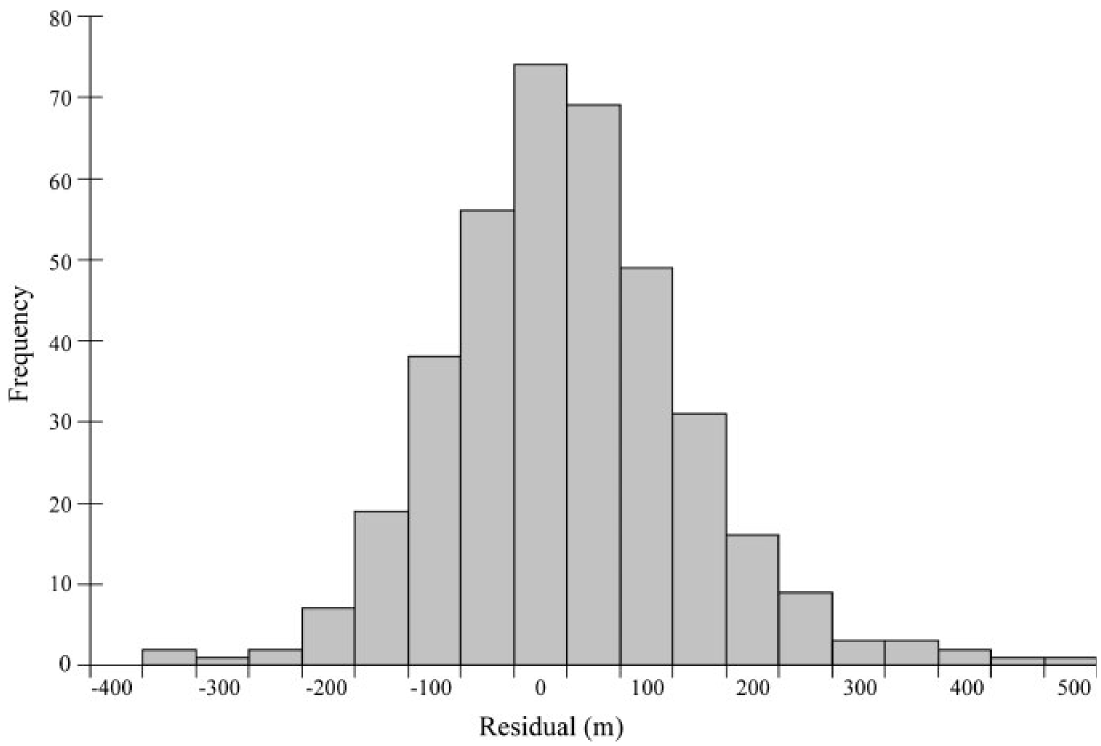

Figure 4 Histogram of residuals above and below the third-order reconstructed equilibrium-line altitude trend surface

Table 3 Least-squares regressions of glacier characteristics against residual values from the third-order reconstructed equilibrium-line altitude trend surface

	Y-intercept	*X* value	R^2	*p*
Slope (°)	12.0	8.18E-03	0.048	1.43E-05
Area (km^2)	2.28	−1.04E-02	0.032	4.63E-04
Volume (km^3)	0.19	−9.93E-04	0.017	9.99E-03
cos (aspect)	0.76	−4.60E-04	0.019	7.06E-03
Compactness	0.41	3.35E-04	0.076	3.89E-08
Maximum elevation (m)	1160	7.00E-01	0.049	1.29E-05

Globally, the average ELA lowering was ca. 1000 m (Broecker and Denton, 1990). The less-than-average ΔELA for Alaska has previously been attributed to a deficiency in moisture during the LGM suggesting drier-than-present conditions (e.g. Porter *et al.*, 1983; Kaufman and Manley, 2004). Relatively gentle ELA gradients also suggest that continental climate conditions prevailed during the LGM. The major trends in the LGM ELA and glaciation thresholds for the Brooks Range, and elsewhere from Alaska, as well as the distribution of cirque-floor elevations (Péwé, 1975), show a strong component of southwesterly moisture flow across the state. In contrast, Pleistocene sand sheets distributed around central and northern Alaska show that wind directions were dominantly northeasterly (Lea and Waythomas, 1990). Evidence from loess deposits also indicates northeasterly winds during the LGM (Muhs *et al.*, 2003). The apparent contradiction between glacial and aeolian evidence may result from differences in surface and upper atmospheric wind regimes. Episodic surface winds are responsible for moving sand and silt to form sand dunes and deposit loess, while perpetual upper-atmospheric, moisture-bearing winds affect storm tracks and control the accumulation on glaciers. Differences in the seasonal pattern of atmospheric circulation could also explain the differences in the proxy records. ELAs are mostly influenced by winter storms that carry moisture that falls as snow, as opposed to the formation of loess and dune deposits that take place during the summer when sediment is unfrozen, snow cover is absent, and barren outwash from summer ablation is abundant (Muhs *et al.*, 2003).

Conclusions

ELA reconstructions from the Brooks Range provide an important proxy for LGM climate trends. LGM ELAs rise from 470 m a.s.l. in the west to 1860 m a.s.l. in the eastern Brook Range. Modelled by a third-order trend surface, palaeo-ELAs lower toward the southwest across most of the range, and toward the northeast in the eastern Brooks Range. The southwestern lowering of ELAs across the range is dominant during the LGM, as it is today, indicating a source of moisture from the northern Pacific Ocean. This interpretation is similar to previous observations (e.g. Porter *et al.*, 1983) and highlights the general stability of the regional atmospheric pressure systems, despite the impact of the Laurentide Ice Sheet on atmospheric circulation to the east (e.g. Bartlein *et al.*, 1998). The northward lowering of LGM ELAs in the northeastern Brooks Range is probably at least in part the result of the cold temperatures where the range is farthest north and closest to the Beaufort Sea.

The residual analysis produced the somewhat unexpected result that smaller glaciers tend to lie above, rather than below, the regional ELA trend surface. Small glaciers might be found at higher elevations because of the drying of rising air masses, or the diversion of moisture around higher elevations. This trend may be a function of an orographic influence on smaller glaciers, although this relationship may not be as strong because of the small range of glaciers sizes represented by this dataset.

LGM ELA lowering relative to modern glacier ELAs is not uniform across the Brooks Range. ELA lowering decreases toward the east from 700 to 200 m. The small amount of ELA depression in the northeastern Brooks Range has been attributed to postglacial uplift (Porter *et al.*, 1983), but might in part be explained by the relatively low ELAs of modern glaciers that presently receive moisture from the Beaufort Sea. The average depression of LGM ELAs in the Brooks Range is similar to other mountain ranges around Alaska and less than the global average lowering. LGM aridity in this region has been attributed to increased sea-ice cover, the exposure of the Bering/Chukchi platform by eustatic sea-level lowering, colder sea-surface temperatures over the moisture source in the northern Pacific Ocean in response to lower global temperatures and increased discharge of glacier ice, and the intensification of the orographic barrier of the Alaska Range associated with the growth of the Cordilleran Ice Sheet (Porter *et al.*, 1983). Furthermore, upper-level wind anomalies simulated for the LGM by general circulation models show a general anticyclonic curvature over Alaska, with a greater tendency for enhanced subsidence and suppression of precipitation (Bartlein *et al.*, 1998).

Apparent contradictions in LGM atmospheric circulation patterns exist among geologic records. The opposing patterns of winds recorded from glacial and aeolian evidence are mostly the result of a difference between upper atmosphere moisture circulation and the generation of surface winds, but may also reflect seasonal differences in wind regimes.

Acknowledgements Our understanding of ELAs and their significance in reconstructing palaeoclimates has been enriched by the outstanding and inspiring research by Geoff Seltzer and his colleagues. This project was funded by National Science Foundation Grants OPP-9977972 and OPP-9977974, and a Geological Society of America graduate research grant. We thank Patrick Bartlein, Lee Dexter, Michael Ort, and two anonymous reviewers for their input, and Rob Richardson, Janelle Sikorski and Jason Briner for assistance in the field. We are also grateful to Thomas Hamilton who shared his aerial photographs and guided our recognition of LGM moraines in the Brooks Range.

References

Allen TR. 1998. Topographic context of glaciers and perennial snowfields, Glacier National Park, Montana. *Geomorphology* **21**: 207–216.

Balascio NL. 2003. *Equilibrium-line altitudes across the Brooks Range, Alaska during the last glacial maximum.* MS thesis, Northern Arizona University.

Balascio NL, Kaufman DS, Briner JP, Manley WF. in press. Late Pleistocene glacial geology of the Okpilak-Kongakut Rivers region, northeastern Brooks Range, Alaska. *Arctic Antarctic and Alpine Research*.

Bartlein PJ, Anderson KH, Anderson PM, Edwards ME, Mock CJ, Thompson RS, Webb RS, Webb T, Whitlock C. 1998. Paleoclimate simulations for North America over the past 21,000 years: features of the simulated climate and comparisons with paleoenvironmental data. *Quaternary Science Reviews* **17**: 549–585.

Benn DI, Owen LA, Osmaston HA, Seltzer GO, Porter SC, Mark B. 2005. Reconstruction of equilibrium-line altitudes for tropical and sub-tropical glaciers. *Quaternary International* **138–139**: 8–21.

Briner JP, Kaufman DS. 2000. Late Pleistocene glaciation of the southwestern Ahklun Mountains, Alaska. *Quaternary Research* **53**: 13–22.

Broecker WS, Denton GH. 1990. The role of ocean–atmosphere reorganizations in glacial cycles. *Quaternary Science Reviews* **9**: 305–343.

Clark DH, Clark MM, Gillespie AR. 1994. Debris-covered glaciers in the Sierra Nevada, California, and their implications for snowline reconstructions. *Quaternary Research* **41**: 139–153.

Daly C, Neilson RP, Phillips DL. 1994. A statistical-topographic model for mapping climatological precipitation over mountainous terrain. *Journal of Applied Meteorology* **33**: 140–158.

Dyurgerov M. 2002. *Glacier mass balance and regime: data of measurements and analysis*. INSTAAR Occasional Paper no. 55, University of Colorado.

Fahl CB. 1975. Mean sea level pressure patterns relating to glacier activity in Alaska. In *Climate of the Arctic*, Weller G, Bowling SA (eds). University of Alaska Geophysical Institute: Fairbanks, AK; 339–346.

Hamilton TD. 1978a. Surficial geologic map of the Chandalar quadrangle, Alaska. US Geological Survey Miscellaneous Field Studies Map, MF-878A.

Hamilton TD. 1978b. Surficial geologic map of the Philip Smith Mountain quadrangle, Alaska. US Geological Survey Miscellaneous Field Studies Map, MF-879A.

Hamilton TD. 1979a. Surficial geologic map of the Chandler Lake quadrangle, Alaska. US Geological Survey Miscellaneous Field Studies Map, MF-1121.

Hamilton TD. 1979b. Surficial geologic map of the Wiseman quadrangle, Alaska. US Geological Survey Miscellaneous Field Studies Map, MF-1122.

Hamilton TD. 1980. Surficial geologic map of the Killik River quadrangle, Alaska. US Geological Survey Miscellaneous Field Studies Map, MF-1234.

Hamilton TD. 1981. Surficial geologic map of the Survey Pass quadrangle, Alaska. US Geological Survey Miscellaneous Field Studies Map, MF-1320.

Hamilton TD. 1984a. Surficial geologic map of the Howard Pass quadrangle, Alaska. US Geological Survey Miscellaneous Field Studies Map, MF-1677.

Hamilton TD. 1984b. Surficial geologic map of the Ambler River quadrangle, Alaska. US Geological Survey Miscellaneous Field Studies Map, MF-1678.

Hamilton TD. 1986. Late Cenozoic glaciation of the central Brooks Range. In *Glaciation in Alaska—The Geologic Record*, Hamilton TD, Reed KM, Thorson RM (eds). Alaska Geological Society: Anchorage, AK; 9–49.

Hamilton TD. 1994. Late Cenozoic glaciation of Alaska. In *The Geology of North America*, Plafker G, Berg HC (eds). Geological Society of America: Boulder, CO: 813–845.

Hamilton TD. 2002a. Surficial geologic map of the Hughes quadrangle, Alaska. US Geological Survey Miscellaneous Field Studies Map, MF-2408.

Hamilton TD. 2002b. Surficial geologic map of the Bettles quadrangle, Alaska. US Geological Survey Miscellaneous Field Studies Map, MF-2409.

Hamilton TD. 2003. *Surficial geology of the Dalton Highway (Itkillik–Sagavanirktok Rivers) area, southern Arctic Foothills, Alaska*. Alaska Department Natural Resources/Division Geological and Geophysical Surveys, Professional Report 121.

Hamilton TD, Porter SC. 1975. Itkillik glaciation in the Brooks Range, northern Alaska. *Quaternary Research* **5**: 471–497.

Hawkins PR. 1985. Equilibrium-line altitudes and paleoenvironment in the Merchants Bay area, Baffin Island, N.W.T., Canada. *Journal of Glaciology* **31**: 205–213.

Haugen RK. 1979. *Climatic investigations along the Yukon River to Prudhoe Bay Haul Road, Alaska, 1975–1978*. Informal extract from Final Federal Highway Administrative Contract Report, Environmental Engineering Investigations along the Yukon River Prudhoe Bay Haul Road, Alaska. US Army Cold Regions Research and Engineering Laboratory: Hanover, NH.

Kaufman DS, Hopkins DM. 1986. Glacial history of the Seward Peninsula. In *Glaciation in Alaska—The Geologic Record*, Hamilton TD, Reed KM, Thorson RM (eds). Alaska Geological Society: Anchorage, AK; 51–78.

Kaufman DS, Manley WF. 2004. Pleistocene maximum and Late Wisconsin glacier extents across Alaska, U.S.A. In *Quaternary Glaciations—Extent and Chronology*, Ehlers J, Gibbard PL (eds). Part II: North America. Developments in Quaternary Science, vol. 2, Elsevier: Amsterdam; 9–27.

Kaufman DS, Manley WF, Forman SL, Layer PW. 2001. Pre-Late-Wisconsin glacial history, coastal Ahklun Mountains, southwestern Alaska—new amino acid, thermoluminescence, and $^{40}Ar/^{39}Ar$ results. *Quaternary Science Reviews* **20**: 337–352.

Lea PD, Waythomas CF. 1990. Late-Pleistocene eolian sand sheets in Alaska. *Quaternary Research* **34**: 269–281.

Leonard EM. 1984. Late Pleistocene equilibrium-line altitudes and modern snow accumulation patterns, San Juan Mountains, Colorado, U.S.A. *Arctic and Alpine Research* **16**: 65–76.

Locke WW. 1990. Late Pleistocene glaciers and the climate of western Montana, U.S.A. *Arctic and Alpine Research* **22**: 1–13.

Manley WF. in press. Geospatial inventory and analysis of glaciers: A case study for the eastern Alaska Range, in Glaciers of Alaska. In *Satellite Image Atlas of Glaciers of the World*, Williams RS, Ferrigno JG (eds). US Geological Survey Professional Paper 1386-K.

Manley WF, Daly C. 2005. *Alaska geospatial climate animations of monthly temperature and precipitation*. INSTAAR, University of Colorado. http://instaar.colorado.edu/QGISL/AGCA

Manley WF, Kaufman DS, Briner JP. 1997. GIS determination of modern and late Wisconsin equilibrium line altitudes in the Ahklun Mountains of southwestern Alaska. In *28th Arctic Workshop*: University of Colorado: Boulder, CO; 107–108.

Mann DH, Peteet DM. 1994. Extent and timing of the last glacial maximum in southwestern Alaska. *Quaternary Research* **42**: 136–148.

Mark BG, Harrison SP, Spessa A, New M, Evans DJA, Helmens KF. 2005. Tropical snowline changes at the last glacial maximum: a global assessment. *Quaternary International* **138–139**: 168–201.

Meierding TC. 1982. Late Pleistocene glacial equilibrium-line altitudes in the Colorado Front Range: a comparison of methods. *Quaternary Research* **18**: 289–310.

Mock CJ, Bartlein PJ, Anderson PM. 1998. Atmospheric circulation patterns and spatial climatic variations in Beringia. *International Journal of Climatology* **10**: 1085–1104.

Muhs DR, Ager TA, Bettis EA, McGeehin Been JM, Begét JE, Pavich MJ, Stafford TW, Stevens D. 2003. Stratigraphy and palaeoclimatic significance of late Quaternary loess–palaeosol sequences of the last interglacial–glacial cycle in central Alaska. *Quaternary Science Reviews* **22**: 1947–1986.

Péwé TL. 1975. *Quaternary geology of Alaska*. US Geological Survey Professional Paper no. 385.

Porter SC. 2001. Snowline depression in the tropics during the Last Glaciation. *Quaternary Science Reviews* **20**: 1067–1091.

Porter SC, Pierce KL, Hamilton TD. 1983. Late Wisconsin mountain glaciation in the western United States. In *Late Quaternary Environments of the United States*, Porter SC (ed.). University of Minnesota Press: Minneapolis, MN; 71–111.

Stilwell KB, Kaufman DS. 1996. Late Wisconsin glacial history of the northern Alaska Peninsula, southwestern Alaska, U.S.A. *Arctic and Alpine Research* **28**: 475–487.

Wendler G, Ishikawa N, Streten N. 1974. The climate of the McCall Glacier, Brooks Range, Alaska, in relation to its geographical setting. *Arctic and Alpine Research* **6**: 307–318.

Wendler G, Benson C, Fahl C, Ishikawa N, Trabant D, Weller G. 1975. Glacio-meteorological studies of McCall Glacier. In *Climate of the Arctic*, Weller G, Bowling SA (eds). University of Alaska Geophysical Institute: Fairbanks, AK; 334–338.

Appendix: Physical characteristics for all reconstructed last glacial maximum valley glaciers

Region	UTM Albers Easting[a]	UTM Albers Northing[a]	Lowest elevation (m)	Highest elevation (m)	Average elevation (m)	Elevation range (m)	Area (km^2)	Perimeter (km)	Compactness	Aspect (°)	Slope (°)	Length (km)	Width (km)	Volume (km^3)	ELA (m)
Eastern Brooks Range	336304	2192999	817	1546	1248	729	3.02	14.4	0.18	4	9	1.9	1.59	0.26	1306
	341427	2185443	772	1494	1102	722	1.68	9.0	0.26	350	15	2.2	0.76	0.12	1037
	340459	2185342	902	1471	1133	569	0.49	4.6	0.29	328	17	1.1	0.44	0.01	1067
	338619	2184197	1026	1352	1225	326	0.27	2.5	0.54	14	20	0.7	0.39	0.01	1235
	401688	2183485	1163	2265	1810	1102	6.71	24.4	0.14	337	11	5.4	1.24	0.52	1709
	466340	2190943	924	1447	1180	523	0.73	4.4	0.47	6	16	1.5	0.49	0.05	1155
	468224	2190420	1012	1621	1379	609	1.16	5.5	0.48	7	16	1.7	0.68	0.12	1374
	474787	2188885	1318	1666	1538	348	0.46	3.4	0.52	352	17	0.9	0.52	0.03	1555
	471575	2184869	1139	1845	1556	706	2.10	9.5	0.29	337	12	2.2	0.95	0.12	1515
	466645	2184069	1219	1825	1540	606	1.50	8.4	0.27	17	11	1.9	0.79	0.10	1501
	470230	2184256	1272	1857	1661	585	1.90	7.2	0.46	320	12	2.3	0.83	0.21	1674
	477233	2185086	1153	1637	1412	484	1.45	5.6	0.57	16	13	1.5	0.96	0.06	1398
	468485	2183364	1240	1857	1604	617	2.12	10.1	0.26	337	12	2.1	1.01	0.16	1598
	472891	2184526	1559	1928	1788	369	0.57	3.6	0.55	345	13	1.1	0.51	0.04	1787
	478891	2184362	1142	1671	1483	529	1.02	4.7	0.58	15	15	1.3	0.78	0.10	1492
	456176	2179967	704	2066	1365	1362	12.39	44.5	0.08	324	9	5.3	2.34	0.92	1288
	480080	2184066	1169	1702	1504	533	0.97	4.6	0.59	3	15	1.4	0.69	0.09	1515
	448433	2179831	1127	1690	1456	563	2.07	8.0	0.40	21	10	2.2	0.94	0.17	1438
	460924	2179498	836	1990	1568	1154	6.83	22.3	0.17	3	10	4.6	1.49	0.80	1555
	493270	2180877	596	2114	1657	1518	7.51	20.9	0.22	13	10	6.1	1.23	1.45	1676
	490959	2181418	822	1859	1543	1037	3.49	12.7	0.27	14	10	3.5	1.00	0.47	1578
	488661	2183090	1027	1268	1177	241	0.38	3.5	0.40	7	9	0.9	0.42	0.01	1179
	468410	2179129	927	2060	1539	1133	9.62	35.3	0.10	333	9	3.7	2.60	0.96	1475
	445551	2175607	973	2017	1645	1044	7.15	21.2	0.20	347	10	5.3	1.35	0.87	1651
	476128	2178246	667	1812	1398	1145	5.93	23.4	0.14	349	10	4.8	1.24	0.57	1397
	463280	2177892	958	2040	1620	1082	4.77	15.4	0.25	17	11	4.9	0.97	0.56	1540
	448343	2177023	1232	1972	1677	740	2.19	10.4	0.25	43	14	2.5	0.88	0.15	1687
	478048	2177965	609	1717	1392	1108	3.11	12.7	0.24	22	10	3.9	0.80	0.25	1411
	471154	2177919	1059	1863	1599	804	3.91	11.8	0.36	35	11	3.0	1.30	0.34	1578
	438252	2174681	1452	1854	1691	402	0.48	3.2	0.57	311	20	0.8	0.59	0.03	1692
	472328	2177146	1210	1832	1626	622	1.01	6.4	0.31	50	13	2.1	0.48	0.05	1635
	479288	2177138	1320	1789	1608	469	0.79	4.9	0.41	6	14	1.4	0.56	0.03	1605
	494586	2178629	1474	2037	1803	563	1.31	5.5	0.54	353	15	1.6	0.82	0.11	1790
	496169	2178670	1514	1845	1721	331	0.60	4.1	0.46	24	10	1.1	0.55	0.03	1724
	495286	2176437	1592	1994	1809	402	0.83	4.3	0.56	21	17	1.1	0.75	0.03	1804
	444189	2170227	1212	1854	1533	642	1.55	7.6	0.34	304	12	2.2	0.70	0.11	1465
	427931	2167906	1225	2139	1754	914	1.79	8.9	0.29	39	13	2.0	0.89	0.14	1733
	433206	2155399	1416	1918	1690	502	1.13	6.7	0.31	344	12	1.5	0.75	0.06	1654
	426346	2153801	1363	1946	1661	583	0.97	6.8	0.26	17	12	1.9	0.51	0.03	1636
	432528	2154852	1575	1977	1814	402	0.67	3.8	0.57	353	13	1.2	0.56	0.05	1819
	427093	2153043	1531	2005	1806	474	0.63	4.3	0.43	5	16	1.2	0.53	0.04	1795
	427890	2153006	1498	2009	1805	511	0.84	4.7	0.48	29	16	1.3	0.65	0.05	1799
	431618	2153567	1647	2000	1855	353	0.43	3.1	0.55	346	16	0.9	0.48	0.02	1859
	428572	2152897	1480	1805	1681	325	0.33	3.0	0.47	36	15	1.0	0.33	0.01	1696

	430391	2153024	1516	2034	1818	518	0.75	4.7	0.43	283	15	1.2	0.63	0.04	1803
	432932	2152629	1298	2123	1750	825	4.27	17.5	0.17	41	9	3.1	1.38	0.32	1726
	429719	2152418	1526	1861	1734	335	0.72	4.1	0.54	346	12	1.1	0.65	0.03	1744
Central Brooks Range	124366	2034078	786	2106	1354	1320	119.52	207.8	0.03	337	5	12.7	9.41	16.70	1297
	132899	2039605	945	2082	1474	1137	14.30	38.5	0.12	346	7	5.3	2.70	1.49	1340
	18181	2038672	1167	2061	1569	894	7.33	24.2	0.16	353	7	6.2	1.18	0.52	1468
	71629	2033107	922	1927	1364	1005	22.38	51.4	0.11	4	5	8.8	2.54	2.32	1265
	84770	2037698	836	1369	1142	533	2.17	10.7	0.24	356	10	2.2	0.99	0.15	1165
	119983	2035923	894	2012	1384	1118	22.56	51.1	0.11	326	7	8.0	2.82	2.07	1347
	130666	2038921	1215	1937	1565	722	3.91	10.8	0.42	263	11	2.9	1.35	0.35	1579
	76742	2031277	891	1891	1394	1000	32.88	96.1	0.04	2	6	9.2	3.57	2.50	1366
	68100	2034306	1142	1483	1356	341	0.40	3.5	0.42	311	15	1.0	0.40	0.02	1369
	74172	2033204	1255	1482	1389	227	1.08	5.8	0.41	297	7	1.6	0.68	0.07	1387
	22780	2015832	1335	1818	1591	483	1.59	7.2	0.39	64	11	2.2	0.72	0.10	1567
	24197	2014246	1066	1691	1398	625	3.52	15.5	0.18	23	9	3.4	1.04	0.24	1408
	27228	2013995	1169	1685	1414	516	2.34	11.8	0.21	7	8	2.6	0.90	0.14	1392
	29377	2012004	1028	1605	1296	577	5.99	25.3	0.12	30	6	3.7	1.62	0.33	1239
	39981	2007223	937	1590	1302	653	1.99	10.7	0.22	348	9	2.4	0.83	0.12	1277
	41667	2007784	1126	1483	1311	357	0.91	5.9	0.33	330	9	1.4	0.65	0.04	1277
	34714	2007381	1037	1504	1340	467	1.05	6.0	0.37	338	11	1.7	0.62	0.08	1376
	41257	2006885	1169	1606	1433	437	1.09	7.1	0.27	8	9	1.6	0.68	0.05	1430
	212026	1971386	1098	1622	1384	524	1.51	7.7	0.32	336	11	2.2	0.69	0.13	1356
	210768	1970299	1274	1657	1496	383	0.42	3.2	0.50	303	19	0.8	0.53	0.02	1497
	220437	1963614	990	1515	1302	525	5.05	14.3	0.31	0	8	3.3	1.53	0.52	1295
	223271	1964004	1244	1612	1462	368	0.83	4.8	0.45	25	10	1.5	0.55	0.05	1466
	224542	1963720	1126	1482	1331	356	1.02	4.9	0.53	12	9	1.6	0.64	0.06	1318
	226477	1963444	1257	1617	1434	360	0.80	4.7	0.46	60	11	1.5	0.53	0.02	1416
	227452	1962501	1097	1585	1381	488	1.74	6.4	0.54	6	10	2.0	0.87	0.13	1388
	229138	1962997	1198	1656	1459	458	0.75	4.0	0.60	20	15	1.1	0.68	0.05	1454
	−157987	1950252	581	853	726	272	0.60	3.7	0.55	356	10	1.0	0.60	0.05	736
	−110907	1951130	711	910	833	199	0.21	2.3	0.50	43	15	0.6	0.34	0.01	840
	−147118	1950160	671	971	772	300	0.39	3.2	0.47	345	14	0.9	0.43	0.01	749
	−148669	1949236	653	955	818	302	0.28	2.5	0.56	35	20	0.6	0.47	0.01	821
	−110445	1949111	628	901	804	273	0.30	3.0	0.41	70	15	0.9	0.33	0.01	812
	−136147	1948100	637	894	774	257	0.31	2.8	0.50	337	19	0.7	0.44	0.02	779
	−134197	1947182	564	900	755	336	1.40	7.7	0.30	348	10	1.5	0.93	0.07	762
	−120976	1947308	603	848	740	245	0.20	2.2	0.53	351	17	0.5	0.40	0.01	747
	−120005	1947027	577	827	740	250	0.29	2.6	0.52	44	14	0.7	0.41	0.01	749
	−119335	1946741	640	868	783	228	0.54	3.5	0.56	46	10	1.1	0.49	0.03	789
	−165688	1946108	582	764	674	182	0.32	2.8	0.53	22	16	0.6	0.53	0.01	678
	−133342	1946721	801	1023	909	222	0.19	2.2	0.51	1	18	0.6	0.32	0.01	906
	−118488	1946697	540	843	698	303	0.52	3.5	0.54	353	13	0.9	0.58	0.03	705
	−135620	1945903	683	923	820	240	0.23	2.2	0.62	335	20	0.5	0.46	0.01	828
	−113567	1945117	456	982	761	526	1.72	7.9	0.34	4	11	2.2	0.78	0.11	751
	−118770	1945678	779	960	882	181	0.30	2.4	0.65	281	12	0.7	0.43	0.02	882
	46799	1947839	1019	1477	1228	458	1.44	6.2	0.46	357	13	1.4	1.03	0.11	1216
	−164806	1944395	569	717	644	148	0.45	3.1	0.58	29	10	0.7	0.64	0.02	640

Continues

Appendix: Continued

Region	UTM Albers Easting[a]	UTM Albers Northing[a]	Lowest elevation (m)	Highest elevation (m)	Average elevation (m)	Elevation range (m)	Area (km^2)	Perimeter (km)	Compactness	Aspect (°)	Slope (°)	Length (km)	Width (km)	Volume (km^3)	ELA (m)
	44628	1947567	1178	1429	1299	251	0.62	3.8	0.52	324	14	1.1	0.56	0.03	1290
	48921	1947274	1028	1434	1189	406	0.96	6.6	0.28	26	10	1.3	0.74	0.05	1134
	43422	1947430	1023	1217	1131	194	0.44	3.2	0.53	310	11	1.0	0.44	0.01	1130
	50442	1946521	1100	1408	1252	308	1.82	8.8	0.30	4	6	2.4	0.76	0.10	1254
	185513	1948351	1070	1516	1338	446	1.64	7.2	0.40	36	8	1.9	0.86	0.16	1331
	186607	1947708	988	1597	1273	609	2.19	9.5	0.31	9	9	2.2	0.99	0.16	1218
	−128879	1943940	654	860	748	206	0.28	2.6	0.51	0	12	0.8	0.35	0.01	741
	−111797	1944194	625	946	814	321	0.57	4.2	0.40	66	13	1.3	0.43	0.02	809
	−128035	1944016	614	834	744	220	0.43	3.4	0.48	48	12	0.9	0.48	0.02	742
	−111057	1943373	548	957	790	409	0.63	5.0	0.31	23	11	1.5	0.42	0.03	806
	52144	1945830	1090	1450	1267	360	0.93	5.0	0.46	28	11	1.6	0.58	0.05	1252
	−134839	1943114	606	816	706	210	0.25	2.4	0.54	358	19	0.5	0.50	0.01	712
	183648	1947731	1218	1636	1417	418	0.43	3.1	0.56	321	22	0.9	0.48	0.01	1393
	197715	1947663	1265	1508	1414	243	0.27	2.4	0.59	333	16	0.6	0.45	0.01	1421
	196636	1946994	1244	1500	1406	256	0.34	2.8	0.56	338	13	0.7	0.49	0.02	1412
	−140119	1941523	517	671	588	154	0.18	2.2	0.49	17	11	0.7	0.26	0.00	590
	54098	1944368	949	1313	1147	364	0.89	5.4	0.38	15	12	1.4	0.64	0.05	1159
	−138774	1940713	467	742	658	275	0.66	4.2	0.47	13	9	1.4	0.47	0.04	680
	−137688	1940734	451	696	605	245	0.44	3.2	0.52	42	12	1.1	0.40	0.02	616
	187835	1945754	1109	1492	1314	383	0.66	4.1	0.50	16	14	1.3	0.51	0.02	1309
	54891	1943842	1087	1276	1211	189	0.39	3.2	0.46	65	9	0.8	0.48	0.02	1222
	−136948	1939972	494	763	674	269	0.44	3.6	0.43	28	11	1.0	0.44	0.02	690
	74432	1941503	565	1202	994	637	3.60	14.2	0.23	6	7	3.2	1.13	0.29	1041
	56474	1942971	996	1334	1187	338	0.68	4.1	0.51	328	14	1.1	0.62	0.05	1186
	−136089	1939272	630	873	747	243	0.24	2.2	0.65	4	18	0.6	0.40	0.01	742
	190209	1943993	1165	1561	1365	396	0.74	4.1	0.56	6	19	1.1	0.67	0.02	1351
	188839	1942306	948	1497	1245	549	6.25	17.3	0.26	299	6	4.2	1.49	0.63	1267
	159444	1941941	983	1502	1229	519	1.44	8.2	0.27	322	10	2.6	0.56	0.07	1184
	161131	1942260	1090	1493	1311	403	0.86	5.5	0.35	359	9	2.0	0.43	0.04	1290
	162753	1942937	1057	1219	1155	162	0.26	2.4	0.57	2	10	0.7	0.37	0.01	1158
	184555	1942075	917	1376	1211	459	1.96	7.4	0.45	328	8	2.8	0.70	0.16	1218
	191613	1942518	781	1370	1165	589	2.67	12.4	0.22	15	10	2.7	0.99	0.24	1168
	158422	1941570	981	1431	1254	450	0.82	5.6	0.33	28	12	1.9	0.43	0.04	1265
	157329	1942093	1017	1390	1206	373	0.50	3.8	0.43	343	15	1.1	0.46	0.02	1183
	186247	1941976	953	1344	1205	391	1.32	6.4	0.41	15	9	2.0	0.66	0.09	1218
	−144197	1937270	644	905	784	261	0.24	2.3	0.58	15	20	0.5	0.48	0.01	786
	−127282	1936572	310	836	646	526	1.44	7.0	0.37	343	10	2.5	0.57	0.09	655
	−119800	1936709	458	901	726	443	1.07	6.1	0.36	3	8	2.3	0.46	0.07	737
	−130179	1936518	306	794	613	488	0.98	5.9	0.36	45	13	2.3	0.43	0.05	629
	−119137	1936722	431	851	706	420	0.89	5.9	0.32	12	9	2.2	0.40	0.05	696
	−129573	1936410	300	757	587	457	0.89	6.1	0.30	349	10	2.0	0.44	0.03	608
	−117808	1936686	470	928	751	458	1.17	6.0	0.41	34	10	2.2	0.53	0.09	755
	−116534	1936352	384	922	690	538	1.69	7.8	0.35	20	9	2.9	0.58	0.12	649
	76440	1940398	943	1264	1140	321	0.66	3.8	0.56	34	13	1.0	0.66	0.04	1141
	−128425	1936372	426	806	649	380	0.74	5.0	0.37	1	11	1.7	0.44	0.04	648

−121246	1936564	540	724	664	184	0.24	2.3	0.57	7	13	0.6	0.40	0.01	678
182696	1941038	1150	1442	1318	292	0.31	2.6	0.56	309	20	0.6	0.52	0.01	1325
77421	1939338	862	1121	1030	259	0.73	4.0	0.58	3	12	1.1	0.66	0.04	1038
156471	1938024	976	1393	1238	417	2.48	9.4	0.36	341	7	2.8	0.89	0.20	1250
75272	1937576	759	1338	1021	579	2.35	9.1	0.35	63	13	1.7	1.38	0.15	1017
−116552	1934203	706	1018	868	312	0.68	4.3	0.46	290	11	1.3	0.53	0.03	870
131869	1935734	783	1434	1176	651	4.81	16.7	0.22	8	8	2.8	1.72	0.57	1199
−111641	1933099	621	995	847	374	0.80	4.4	0.51	35	12	1.1	0.72	0.05	847
147608	1937134	913	1321	1167	408	0.64	4.0	0.51	4	17	1.1	0.58	0.05	1184
−129121	1931943	396	798	625	402	0.97	5.8	0.37	9	10	1.6	0.61	0.05	612
133986	1935404	919	1461	1214	542	2.34	8.6	0.39	64	12	2.4	0.97	0.23	1207
−118350	1930470	405	996	741	591	3.60	15.1	0.20	356	7	3.9	0.92	0.23	717
129826	1934991	903	1267	1090	364	1.38	7.1	0.35	35	9	2.3	0.60	0.07	1080
136220	1935434	913	1249	1123	336	0.79	4.3	0.53	359	11	1.2	0.66	0.07	1137
−130907	1930716	494	803	696	309	0.82	5.4	0.36	315	9	1.6	0.52	0.05	699
−121199	1931134	630	847	769	217	0.22	2.2	0.59	12	15	0.6	0.37	0.01	781
−115673	1929385	388	980	710	592	3.32	13.1	0.24	59	7	3.6	0.92	0.23	667
61557	1933975	1031	1276	1144	245	0.32	2.5	0.64	9	16	0.7	0.46	0.01	1140
−116304	1930806	651	965	829	314	0.49	3.6	0.47	56	14	1.1	0.44	0.02	820
−119741	1930624	697	944	848	247	0.30	2.9	0.45	19	13	0.7	0.43	0.01	852
63137	1933282	963	1253	1101	290	0.40	3.0	0.56	347	18	0.8	0.50	0.02	1104
−131665	1929389	305	782	562	477	1.21	7.6	0.27	341	11	2.2	0.55	0.07	567
−127314	1929052	532	812	730	280	0.75	4.1	0.56	357	10	1.3	0.57	0.05	757
−128578	1928909	482	764	662	282	0.68	4.2	0.48	27	12	1.3	0.52	0.04	671
−118850	1928312	516	872	721	356	2.23	9.5	0.31	292	6	2.8	0.80	0.08	705
−127911	1925699	457	748	635	291	0.52	3.8	0.44	19	12	1.1	0.47	0.03	641
81393	1927338	708	1116	937	408	0.48	3.4	0.54	333	21	1.0	0.48	0.03	933
82733	1926462	794	1133	1024	339	0.69	4.1	0.52	22	13	1.1	0.63	0.04	1020
80925	1926257	809	1203	1085	394	0.74	4.4	0.47	329	13	1.3	0.57	0.06	1121
−116538	1921192	487	873	708	386	1.27	6.2	0.41	63	10	1.8	0.71	0.08	704
64507	1922019	676	1199	936	523	5.32	16.8	0.24	15	5	4.0	1.33	0.29	927
79871	1923973	826	1217	1042	391	0.80	4.3	0.54	26	14	1.2	0.67	0.05	1027
62519	1921752	682	1149	902	467	5.85	15.8	0.29	339	5	4.6	1.27	0.27	891
−115503	1920673	514	828	713	314	0.64	3.8	0.55	27	14	1.1	0.58	0.04	713
60053	1921178	598	1180	893	582	7.43	23.2	0.17	314	6	4.5	1.65	0.35	882
−71679	1919841	474	1062	844	588	0.69	4.7	0.40	338	18	1.3	0.53	0.04	844
58558	1920260	588	1110	912	522	2.70	11.8	0.25	319	10	3.6	0.75	0.14	906
9627	1919156	447	1067	847	620	2.87	12.1	0.25	347	7	2.6	1.10	0.22	871
−104183	1918789	591	939	763	348	1.48	7.3	0.35	272	7	1.7	0.87	0.07	731
−72377	1918456	565	1240	936	675	2.08	9.1	0.31	352	10	2.3	0.91	0.20	912
6698	1917378	520	1178	888	658	6.96	24.5	0.15	324	7	3.7	1.88	0.56	868
−74998	1916559	551	1279	897	728	2.75	12.6	0.22	2	8	4.3	0.64	0.17	825
45732	1918278	553	1194	928	641	8.67	28.8	0.13	10	7	4.4	1.97	0.57	911
−105550	1917690	515	857	750	342	1.41	7.6	0.31	285	9	2.2	0.64	0.06	790
−73928	1917474	576	1154	873	578	1.99	10.0	0.25	326	9	2.9	0.69	0.11	853
11371	1919542	481	1073	816	592	0.76	5.3	0.34	18	14	1.2	0.64	0.05	811
−84481	1917110	703	1187	1001	484	2.26	10.1	0.28	103	11	2.2	1.03	0.16	1009

Continues

Appendix: Continued

Region	UTM Albers Easting[a]	UTM Albers Northing[a]	Lowest elevation (m)	Highest elevation (m)	Average elevation (m)	Elevation range (m)	Area (km^2)	Perimeter (km)	Compactness	Aspect (°)	Slope (°)	Length (km)	Width (km)	Volume (km^3)	ELA (m)
	−106798	1916712	453	969	752	516	2.90	10.3	0.34	314	8	2.8	1.04	0.20	740
	−76742	1916230	465	1243	903	778	3.15	12.2	0.26	329	10	3.2	0.99	0.24	883
	65924	1920070	930	1145	1053	215	0.62	4.0	0.49	0	9	1.1	0.56	0.03	1066
	−4959	1917969	464	976	817	512	1.49	6.7	0.41	349	10	2.3	0.65	0.11	841
	−108421	1916384	439	803	699	364	0.76	4.7	0.43	324	10	1.3	0.58	0.04	731
	−6752	1916866	477	1077	859	600	3.38	11.6	0.31	28	8	2.9	1.17	0.37	832
	51472	1917826	467	1084	868	617	2.14	9.8	0.28	10	9	3.0	0.71	0.18	901
	−8622	1916836	523	1141	875	618	2.38	9.1	0.36	8	9	2.8	0.85	0.21	866
	52308	1918436	498	1032	798	534	0.88	5.5	0.36	337	14	1.7	0.52	0.05	793
	64718	1915813	465	1244	841	779	8.53	22.9	0.20	183	5	4.3	1.98	0.58	703
	−87322	1914134	315	1185	858	870	14.18	47.6	0.08	110	8	4.0	3.55	1.11	875
	66433	1918226	701	1219	993	518	2.48	11.4	0.24	166	9	3.2	0.78	0.07	980
	48268	1918197	651	1168	908	517	1.65	8.8	0.27	354	12	2.0	0.82	0.07	885
	49605	1917560	589	1137	918	548	2.22	9.2	0.33	6	8	2.6	0.85	0.16	925
	50501	1918170	506	1040	841	534	0.69	5.0	0.34	17	14	1.5	0.46	0.05	865
	439	1916324	302	1168	673	866	13.23	38.9	0.11	309	7	5.4	2.45	0.72	552
	−78959	1915416	392	1081	784	689	2.61	10.8	0.28	272	10	2.6	1.01	0.16	833
	−15194	1916431	701	1287	1077	586	4.40	13.4	0.31	123	8	3.0	1.47	0.35	1101
	−79958	1913965	362	1048	869	686	1.83	9.1	0.28	328	10	2.2	0.83	0.16	919
	9626	1915454	544	1121	902	577	2.64	11.4	0.25	37	9	2.6	1.01	0.15	923
	9991	1911459	405	1282	858	877	27.11	69.7	0.07	16	5	8.5	3.19	2.41	835
	−81148	1913048	496	1024	855	528	1.31	7.1	0.33	308	10	2.0	0.65	0.10	872
	−82458	1912130	367	1061	733	694	1.74	9.2	0.26	324	11	2.8	0.62	0.10	718
	−90283	1911156	543	1084	885	541	3.51	16.1	0.17	102	10	2.7	1.30	0.21	887
	−83633	1910437	295	1087	699	792	4.52	15.8	0.23	286	8	3.0	1.51	0.25	578
	−76218	1910746	690	1146	927	456	0.90	5.3	0.41	13	13	1.6	0.56	0.05	905
	3920	1910049	424	1159	831	735	7.21	22.9	0.17	313	6	4.7	1.53	0.60	867
	5728	1910137	607	1228	857	621	3.57	15.0	0.20	324	7	2.9	1.23	0.19	813
	17866	1909551	530	1178	922	648	4.57	14.3	0.28	358	6	4.7	0.97	0.46	943
	−61173	1909453	673	1188	1034	515	1.79	7.8	0.37	37	10	2.2	0.81	0.20	1068
	14913	1909326	607	1286	933	679	8.16	24.4	0.17	356	7	4.0	2.04	0.54	915
	−62388	1909910	829	1223	1029	394	1.21	5.8	0.46	24	14	1.6	0.75	0.06	1020
	20035	1909764	479	1172	909	693	3.70	12.4	0.30	17	7	3.1	1.19	0.43	899
	−75285	1909210	619	1112	912	493	1.59	7.4	0.36	40	12	1.9	0.84	0.11	919
	−60073	1908696	553	1112	862	559	2.21	10.3	0.26	39	10	3.2	0.69	0.16	839
	−57526	1907963	428	1112	845	684	2.82	11.8	0.26	44	10	2.6	1.08	0.25	834
	−58676	1908182	550	1074	867	524	1.94	9.4	0.28	66	9	2.2	0.88	0.15	844
	−74245	1908392	619	1022	877	403	1.31	6.2	0.42	61	11	1.6	0.82	0.11	899
	−25916	1908194	583	1087	885	504	1.06	5.8	0.40	18	11	2.0	0.53	0.07	881
	−20061	1907991	431	981	773	550	1.32	5.9	0.48	354	12	1.8	0.73	0.10	793
	−21204	1907793	501	983	816	482	1.29	6.4	0.40	21	10	1.9	0.68	0.09	831
	2071	1908706	653	1071	925	418	1.40	7.0	0.36	298	8	2.1	0.67	0.09	915
	−22356	1908133	689	1001	897	312	0.80	4.4	0.51	10	9	1.3	0.61	0.05	908
	−92501	1907175	663	929	823	266	0.39	2.9	0.58	23	15	0.8	0.48	0.02	829
	8116	1907965	850	1135	1039	285	0.92	4.9	0.48	140	8	1.3	0.71	0.05	1049

−28774	1905937	564	1092	915	528	2.97	10.0	0.38	348	7	3.1	0.96	0.31	941
9263	1907923	1015	1232	1155	217	0.34	2.9	0.52	149	11	0.7	0.49	0.02	1170
7102	1907232	916	1204	1103	288	0.53	3.6	0.51	155	12	1.0	0.53	0.03	1113
6081	1906977	977	1247	1127	270	0.29	2.5	0.58	175	17	0.7	0.42	0.01	1122
−27084	1905905	842	1119	1022	277	0.45	3.7	0.41	72	15	1.0	0.45	0.02	1034
19136	1905509	604	1048	838	444	1.31	6.2	0.42	20	10	1.7	0.77	0.08	824
20105	1905286	571	971	806	400	1.02	5.4	0.44	0	10	1.7	0.60	0.06	816
21012	1905180	569	958	822	389	0.93	5.3	0.42	342	10	1.6	0.58	0.05	845
206856	1899359	850	1629	1196	779	9.10	22.7	0.22	36	6	6.5	1.40	0.93	1145
−88424	1892314	420	864	694	444	0.87	4.8	0.48	9	15	1.4	0.62	0.09	713
−85684	1890868	412	855	671	443	2.94	11.3	0.29	33	8	2.9	1.02	0.23	689
−83059	1892408	668	852	778	184	0.17	1.9	0.59	333	15	0.5	0.35	0.01	785
−75874	1891876	642	1005	812	363	1.11	5.4	0.48	28	10	1.6	0.69	0.08	781
−86722	1891567	478	917	724	439	0.93	6.4	0.29	75	14	1.9	0.49	0.06	697
−83835	1891976	632	968	804	336	0.39	2.9	0.59	4	21	0.7	0.56	0.03	803
186544	1893558	820	1286	1082	466	3.31	12.8	0.25	20	6	3.9	0.85	0.21	1103
−89784	1890856	513	966	786	453	0.26	2.4	0.56	357	30	0.6	0.43	0.02	809
−83809	1890543	613	914	753	301	1.03	6.4	0.32	44	8	1.7	0.61	0.06	747
−82950	1889781	458	953	642	495	1.12	6.5	0.34	38	11	1.5	0.75	0.08	620
−90430	1889948	526	870	736	344	0.37	2.9	0.56	327	19	0.9	0.41	0.02	743
−90839	1889224	476	1090	835	614	0.81	4.6	0.49	348	23	1.3	0.62	0.13	830
−86172	1887932	607	980	781	373	1.95	8.2	0.37	249	8	2.4	0.81	0.07	762
−87569	1888505	707	932	849	225	0.45	3.2	0.54	314	12	0.9	0.50	0.02	859
188249	1892026	934	1348	1170	414	1.36	6.1	0.46	23	10	1.9	0.71	0.08	1163
−73823	1888506	530	930	697	400	0.36	2.8	0.59	353	25	0.7	0.51	0.03	679
−88465	1888011	721	967	855	246	0.32	2.6	0.58	316	15	0.7	0.46	0.02	854
−75505	1888178	616	953	793	337	0.22	2.3	0.54	19	27	0.5	0.45	0.02	785
−88573	1887352	639	1029	855	390	0.45	3.2	0.54	315	22	1.0	0.45	0.04	856
−84347	1887068	557	918	792	361	1.30	6.2	0.42	78	10	1.9	0.68	0.12	809
−68135	1887410	591	935	743	344	0.32	2.9	0.48	1	17	0.8	0.40	0.02	725
−60048	1887011	612	952	763	340	0.39	4.0	0.31	337	13	1.1	0.35	0.02	753
−65591	1886736	573	1129	850	556	0.73	4.4	0.46	354	28	1.2	0.61	0.08	830
−85782	1886385	788	993	915	205	0.32	2.5	0.63	207	14	0.6	0.53	0.01	921
−60704	1886581	696	925	820	229	0.15	1.8	0.57	282	22	0.5	0.30	0.00	831
−57626	1886395	612	931	801	319	0.36	3.0	0.50	12	18	0.7	0.51	0.02	807
−75826	1885962	667	937	807	270	0.52	3.6	0.50	34	13	1.0	0.52	0.03	807
−63710	1886111	539	911	727	372	0.48	3.4	0.54	349	22	0.8	0.60	0.03	721
−66958	1885637	700	1030	933	330	0.87	4.4	0.56	9	9	1.4	0.62	0.09	955
−62624	1886070	643	855	766	212	0.32	2.6	0.58	10	15	0.7	0.46	0.02	783
−58768	1886196	750	940	867	190	0.29	2.8	0.48	22	19	0.8	0.36	0.01	884
−77511	1885753	644	1046	851	402	0.69	4.0	0.55	319	16	1.1	0.63	0.05	833
−51773	1886136	652	1051	891	399	0.45	3.4	0.50	31	19	0.9	0.50	0.04	903
−60515	1886106	743	959	876	216	0.17	1.9	0.59	301	19	0.5	0.35	0.01	889
−76642	1884394	715	1022	903	307	1.23	5.9	0.45	195	8	2.2	0.56	0.10	902
−75566	1884891	695	1004	861	309	0.82	5.2	0.39	120	8	1.2	0.68	0.05	858
−79305	1884945	714	985	874	271	0.46	3.2	0.55	302	15	1.0	0.46	0.03	875
−78209	1884367	689	1154	902	465	1.52	7.2	0.37	240	10	2.1	0.73	0.12	896

Continues

Appendix: Continued

Region	UTM Albers Easting[a]	UTM Albers Northing[a]	Lowest elevation (m)	Highest elevation (m)	Average elevation (m)	Elevation range (m)	Area (km^2)	Perimeter (km)	Compactness	Aspect (°)	Slope (°)	Length (km)	Width (km)	Volume (km^3)	ELA (m)
Western Brooks Range	−257751	2081572	1148	1376	1280	228	0.29	2.6	0.53	17	16	0.6	0.49	0.01	1278
	−258927	2078800	913	1134	1052	221	0.22	2.0	0.67	39	17	0.5	0.45	0.01	1059
	−340691	2073305	449	774	623	325	0.61	4.8	0.33	331	10	1.6	0.38	0.02	614
	−343227	2072655	462	857	646	395	2.80	16.4	0.13	353	8	3.0	0.93	0.10	606
	−279575	2068233	879	1084	984	205	0.21	2.2	0.57	354	19	0.5	0.42	0.01	997
	−280347	2067634	812	1046	959	234	0.55	4.0	0.44	13	11	1.1	0.50	0.03	969
	−281897	2066377	686	1077	884	391	0.56	4.0	0.45	317	16	1.1	0.51	0.03	855
	−348990	2070152	438	872	591	434	3.67	19.3	0.12	35	6	3.8	0.97	0.13	549
	−275574	2060604	467	1254	807	787	8.52	33.6	0.09	317	7	5.3	1.61	0.53	797
	−351921	2067325	515	845	714	330	0.88	5.5	0.36	316	10	1.7	0.52	0.04	712
	−270658	2060538	590	1205	873	615	4.78	16.3	0.23	6	8	2.9	1.65	0.31	828
	−353933	2066338	441	819	620	378	0.85	5.8	0.32	324	11	1.6	0.53	0.03	605
	−185697	2051066	578	1204	793	626	9.07	25.8	0.17	343	4	3.8	2.39	0.34	717
	−269493	2059021	640	1066	879	426	1.85	10.8	0.20	42	8	1.6	1.15	0.03	837
	−273559	2057414	638	1115	903	477	6.09	21.7	0.16	88	6	3.3	1.85	0.42	887
	−277150	2057322	622	1157	923	535	5.57	17.2	0.24	294	7	2.8	1.99	0.48	891
	−355793	2063193	564	837	734	273	0.87	5.8	0.33	332	7	1.6	0.54	0.05	747
	−325914	2060725	643	1017	828	374	0.71	4.0	0.57	356	13	1.1	0.64	0.06	826
	−178185	2049183	542	1019	797	477	4.10	13.6	0.28	135	5	3.5	1.17	0.28	789
	−181574	2047771	491	1102	749	611	10.26	30.0	0.14	144	5	6.3	1.63	0.60	742
	−189833	2049412	894	1063	985	169	0.39	3.0	0.55	340	9	0.8	0.49	0.01	988
	−188081	2049279	887	1051	983	164	0.25	2.3	0.60	354	11	0.6	0.41	0.00	985
	−273376	2052451	527	1161	808	634	11.88	26.3	0.22	110	4	5.7	2.08	1.07	745
	−280391	2052016	510	1223	809	713	10.91	29.0	0.16	243	5	5.9	1.85	0.86	729
	−326927	2056744	751	1092	894	341	0.67	3.8	0.57	326	15	1.0	0.67	0.05	875
	−327906	2056637	609	1035	829	426	0.84	4.7	0.48	327	12	1.5	0.56	0.04	817
	−325670	2055639	635	952	794	317	1.75	7.6	0.38	109	10	1.6	1.09	0.10	799
	−294891	2049686	319	928	637	609	2.75	14.6	0.16	306	9	3.0	0.92	0.12	611
	−319993	2051825	601	906	779	305	0.67	3.6	0.65	31	14	1.0	0.67	0.03	779
	−292997	2049009	839	1089	991	250	0.49	3.2	0.58	17	15	0.8	0.61	0.02	996
	−332276	2051528	674	960	813	286	0.37	3.8	0.31	331	13	1.1	0.33	0.01	814
	−329609	2050618	483	946	653	463	2.70	11.4	0.26	359	9	3.1	0.87	0.10	604
	−291293	2047393	456	929	661	473	6.57	21.0	0.19	67	4	3.8	1.73	0.31	637
	−335344	2050201	641	849	750	208	0.46	3.5	0.48	287	12	1.0	0.46	0.02	751
	−336271	2049970	760	958	840	198	0.33	3.1	0.42	289	12	0.9	0.36	0.01	822
	−328490	2049284	483	877	681	394	1.13	5.9	0.41	33	12	1.9	0.59	0.06	663
	−331599	2049093	607	924	743	317	0.53	4.2	0.38	311	18	1.0	0.53	0.01	730
	−334398	2048999	520	788	651	268	1.30	6.2	0.42	85	6	1.9	0.69	0.06	622
	−295356	2045783	732	1094	903	362	0.98	5.4	0.42	300	10	1.6	0.61	0.04	886
	−328381	2048262	529	798	670	269	0.37	4.0	0.29	50	10	0.8	0.46	0.01	666
	−328776	2046979	746	901	817	155	0.14	1.8	0.56	16	16	0.5	0.29	0.00	819
	−268675	2040351	457	893	652	436	5.65	18.2	0.21	26	5	4.5	1.26	0.32	584
	−271988	2039881	658	900	790	242	0.45	3.2	0.54	337	14	0.8	0.57	0.02	790
	−274805	2039553	573	734	670	161	0.25	2.3	0.60	333	12	0.5	0.50	0.01	675
	−229272	1981929	929	1190	1111	261	0.46	3.4	0.52	12	11	0.9	0.52	0.04	1129

−230723	1981979	947	1253	1145	306	0.35	3.0	0.49	28	15	0.9	0.39	0.02	1158
−232003	1981895	983	1176	1118	193	0.24	2.3	0.57	341	13	0.7	0.34	0.01	1130
−228232	1981254	852	1160	1040	308	0.45	3.2	0.53	4	15	0.8	0.56	0.04	1041
−229719	1980827	917	1184	1070	267	0.48	3.2	0.57	221	14	0.9	0.53	0.01	1069
−310356	1984365	663	1074	843	411	0.58	4.0	0.47	55	16	1.1	0.53	0.02	820
−306581	1983789	681	939	826	258	0.34	2.8	0.56	20	15	0.7	0.48	0.02	826
−310097	1982911	630	895	771	265	0.56	3.6	0.54	43	11	1.1	0.51	0.03	767
−314324	1976406	532	917	711	385	1.37	6.4	0.43	330	10	2.0	0.69	0.10	686
−310176	1975982	613	887	755	274	0.33	2.9	0.50	9	14	0.9	0.37	0.01	746
−302421	1975173	545	896	726	351	0.24	2.4	0.53	16	22	0.6	0.41	0.01	720
−309194	1975312	584	903	738	319	0.37	2.9	0.56	347	17	0.8	0.46	0.02	732
−310942	1974604	526	916	721	390	0.39	3.5	0.40	42	17	0.9	0.43	0.01	709
−317396	1974121	541	869	751	328	0.39	3.4	0.43	286	12	1.1	0.35	0.02	762
−211498	1966062	717	944	845	227	0.14	1.7	0.61	11	24	0.4	0.34	0.01	856
−310279	1972044	415	910	661	495	0.96	5.5	0.39	34	13	1.7	0.56	0.07	635
−203652	1963256	541	678	602	137	0.36	3.1	0.47	351	9	1.1	0.33	0.01	601
−304647	1970374	517	769	656	252	0.30	2.5	0.59	28	17	0.7	0.43	0.01	651
−213875	1960261	506	631	571	125	0.23	2.0	0.71	24	11	0.5	0.47	0.01	574
−205715	1959226	564	808	679	244	0.37	3.1	0.47	333	17	0.7	0.52	0.02	676
−204169	1958032	520	725	622	205	0.20	2.4	0.43	328	29	0.5	0.40	0.00	626
−187464	1954672	527	771	676	244	0.22	2.3	0.52	17	19	0.5	0.43	0.01	694
−201566	1955622	518	735	638	217	0.23	2.5	0.46	341	23	0.7	0.33	0.00	647
−212063	1956176	559	868	717	309	0.17	2.0	0.51	11	23	0.5	0.34	0.00	724
−186532	1954182	532	726	636	194	0.40	3.0	0.55	21	11	0.9	0.44	0.02	643
−183732	1952773	592	827	720	235	0.47	3.1	0.61	26	12	0.9	0.52	0.02	723
−188958	1953349	413	780	602	367	0.59	4.8	0.32	348	24	0.6	0.98	0.03	598
−200057	1953952	507	705	627	198	0.32	2.9	0.49	339	18	0.8	0.40	0.01	632
−182170	1951816	495	783	633	288	1.83	6.5	0.55	21	6	1.9	0.96	0.12	622
−158000	1950270	581	849	721	268	0.58	3.5	0.60	344	11	1.0	0.58	0.04	728
−180594	1951038	542	678	609	136	0.37	3.0	0.52	359	10	0.7	0.53	0.01	609
−179468	1950713	587	751	678	164	0.35	2.8	0.58	350	9	0.8	0.44	0.01	672
−190377	1951423	385	803	616	418	1.36	6.7	0.38	343	19	1.6	0.85	0.09	622
−212018	1952762	587	778	684	191	0.31	2.5	0.61	346	11	0.7	0.44	0.02	686
−178985	1949899	535	780	695	245	1.23	5.5	0.51	24	8	1.7	0.73	0.08	720
−198806	1951285	341	643	474	302	0.52	3.4	0.58	337	17	0.9	0.58	0.03	468
−225077	1952251	548	833	689	285	0.92	4.7	0.53	5	9	1.3	0.71	0.06	681
−176469	1948750	633	810	725	177	0.41	2.9	0.62	340	13	0.7	0.59	0.02	726
−207576	1950632	479	681	562	202	0.26	2.5	0.51	326	14	0.7	0.37	0.01	553
−209014	1949245	360	671	497	311	0.98	5.3	0.44	350	10	1.4	0.70	0.05	468
−192080	1948142	426	774	585	348	0.44	3.0	0.61	336	18	0.8	0.55	0.03	570
−165708	1946133	583	758	675	175	0.32	2.6	0.58	14	16	0.6	0.53	0.01	676
−209888	1948892	307	667	492	360	1.16	5.8	0.44	310	9	1.6	0.73	0.05	475
−168695	1945883	564	753	671	189	0.84	4.4	0.53	312	7	1.3	0.65	0.06	673
−166509	1945955	640	796	723	156	0.23	2.3	0.56	321	15	0.5	0.46	0.01	726
−167370	1945781	665	816	732	151	0.40	3.2	0.48	9	10	0.9	0.44	0.01	730
−207595	1948779	444	640	540	196	0.52	3.8	0.44	358	11	1.0	0.52	0.02	534
−226418	1949719	517	767	634	250	0.55	3.6	0.53	344	11	1.0	0.55	0.03	630
−220956	1949069	449	736	569	287	0.45	3.2	0.54	342	16	0.8	0.56	0.03	553

Continues

Appendix: Continued

Region	UTM Albers Easting[a]	UTM Albers Northing[a]	Lowest elevation (m)	Highest elevation (m)	Average elevation (m)	Elevation range (m)	Area (km^2)	Perimeter (km)	Compactness	Aspect (°)	Slope (°)	Length (km)	Width (km)	Volume (km^3)	ELA (m)
	−176757	1945780	470	787	628	317	0.58	3.7	0.53	13	17	1.0	0.58	0.04	620
	−206824	1947763	433	717	545	284	0.54	4.0	0.43	9	14	1.1	0.49	0.02	529
	−164812	1944389	567	729	637	162	0.44	3.1	0.56	19	9	0.8	0.54	0.01	635
	−171790	1943426	424	666	549	242	0.69	4.0	0.55	5	9	1.1	0.63	0.04	542
	−266627	1946384	543	772	660	229	0.48	3.1	0.62	357	13	0.8	0.60	0.01	663
	−268086	1945475	708	1010	847	302	0.88	4.7	0.50	339	12	1.3	0.68	0.02	821
	−175072	1926677	536	703	603	167	0.86	4.4	0.55	8	7	1.1	0.78	0.04	594
	−176867	1926156	424	601	517	177	0.65	4.3	0.44	322	10	1.0	0.65	0.02	517
	−268827	1932183	431	723	606	292	1.62	6.5	0.48	14	7	1.9	0.85	0.09	605
	−180199	1926110	511	707	607	196	0.26	2.3	0.62	28	18	0.5	0.51	0.01	609
	−173057	1925326	516	665	587	149	0.22	2.3	0.52	12	11	0.6	0.36	0.01	586
	−177963	1925281	533	703	614	170	0.38	2.8	0.62	334	13	0.7	0.54	0.02	613
	−172482	1924923	537	659	591	122	0.21	2.0	0.63	16	12	0.5	0.42	0.00	589
	−171166	1923146	496	638	553	142	0.17	1.9	0.59	346	12	0.5	0.35	0.01	550
	−170152	1922949	503	687	587	184	0.49	3.2	0.59	13	11	0.8	0.62	0.03	573

[a]Easting and Northing coordinates are presented in the Alaska Albers projection and NAD27 datum.